bulk solids handling Volume 3, Number 1, March 1983

Stress and Wear of Conveyor Belts by Loading Point Impact

H. Ballhaus, Germany

Summary

Loading point impact is one of the main reasons for belt wear. Impulse forces have been determined under realistic operating conditions. Stresses and deformations in the cross-section of a steelcord belt, with and without breaker plies, have been calculated by Finite-Element and Finite-Difference Methods. The non-linear elasticity of rubber has been taken into account. A clear relationship between distribution of stress and belt type is shown. Semi-stochastic impact is simulated in a test stand. First results indicate a strong coincidence of service-life and belt design and almost no relationship with quality standards of the covers.

A technological grade of wear is introduced to establish a rating of test stand results for different belt types.

1. Introduction

The present article is an extract from the Dissertation by the author.* For reasons of space some parts of the Dissertation, dealing with the calculation of time-dependent deformations, the design criteria of a belt wear test stand and the results of a variety of quality tests are not reported here.

Discussed in the following are the main influences of dynamic forces at loading point, the distribution of stresses in the cross-section of different belt types, calculated by two different numerical methods, Finite-Elements and Finite-Differences, the experimental deduction of a specific abrasivity of different materials, first results obtained from a newly designed conveyor belt wear test stand and the deduction of a technological grade of wear.

2. Loading Point Impulse Forces

Problems, occurring during the numerical calculation of the forces when a lump strikes a belt and the far reaching simplifications, under which these impulse forces have been measured [1,2], underline that own data, obtained from a real conveyor, are needed to supplement calculations. Loading point impulse forces, as a function of time, depend heavily on a variety of parameters: belt support, idler spacing, initial tension of the belt, inertial moments of idlers and pulleys, elastic and damping characteristics of the carcass and the covers, of the belt speed, specific weight, geometrical shape, roughness and height of fall of the material are all of importance [3]. For a better knowledge of the loading process with regard to these influences, the impulse forces on a lumpy test object, dropped in free fall onto the running belt, have been determined. Complete results of the investigation, conducted to show precisely the effects of belt speed, height of fall, initial tension and thickness of a damping layer of different materials, on the direction and value of the resulting acceleration of the test object, have been published previously [4]. As an example, Fig. 1 shows a diagram in which

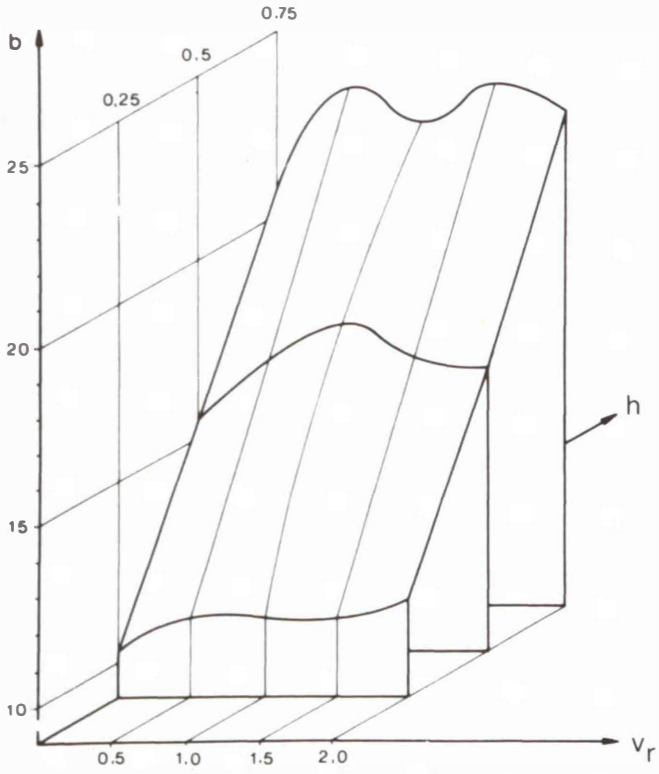

Fig. 1: Maximum acceleration of a test objects as function of height of fall and belt speed

* The Dissertation has been approved by the Faculty of Mechanical Engineering at the University Karlsruhe. The complete Dissertation has been published by the Institut für Fördertechnik and can be ordered by writing to P.O. Box 6380, 7500 Karlsruhe 1, Federal Republic of Germany ("Wissenschaftliche Berichte des Instituts für Fördertechnik", ISSN 0171—2772, No. 8, 183 pages).

the vectorial added maximum acceleration is given as a function of height of fall h and relative belt velocity v_r. Even if the diagram is exact only for a steel cord belt, type ST 630 under initial tension of 45 N/mm, similiar tendencies will be found with other belt types and test objects.

3. Stresses and Deformations in the Cross-Section of a Belt by Concentrated Vertical Forces

3.1 Elasticity of Rubber Used in Belting

Stress-strain-diagrams, according to the specifications of DIN 53 504 [5], show a non-linear elasticity of rubber and indicate a monotonic decrease of the elasticity modulus for strains less than 200 % and a montonic increase above.

Depending on the sign of tension, stress-strain-diagrams differ completely [6—8]. So-called shape factors are widely used [9], to provide a linear elasticity modulus. For limited strains a correction formula is given in [10], which allows one to calculate the deformation of a rubber cylinder by the use of a constant elasticity modulus.

With the basic cross-section F_o it reads:

$$E = \frac{P}{F_o} \quad \frac{1 \pm \epsilon}{\epsilon} \doteq \frac{P}{F_o}\left(\pm \frac{\alpha}{\alpha - 1}\right)$$

To counter the geometric non-linearity caused by contraction of test pieces, tests of tensile strength have been conducted with simultaneously recorded elongations in three directions. For every load level the actual cross-section is given by these results. The resulting stress-strain diagram, Fig. 2, shows, that for at least $\epsilon \leq 60\,\%$, a constant elasticity modulus exists for rubber qualities M and N, DIN 22 131 [11], used in belting.

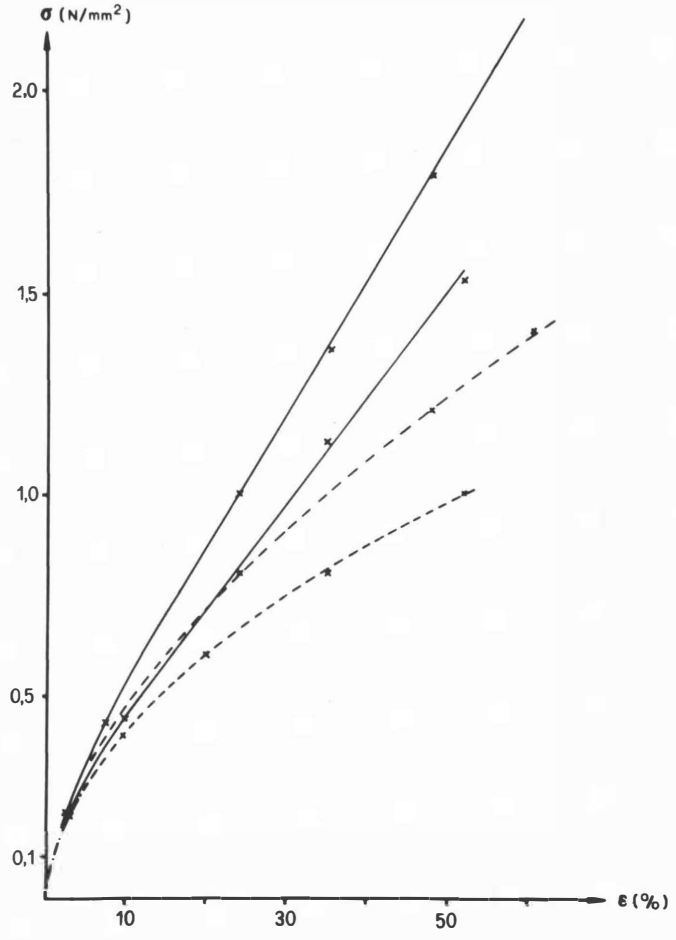

Fig. 2: Stress-strain diagram of tensile strength test for load-dependent cross-section

Fig. 3: Profiles of concentrated loads

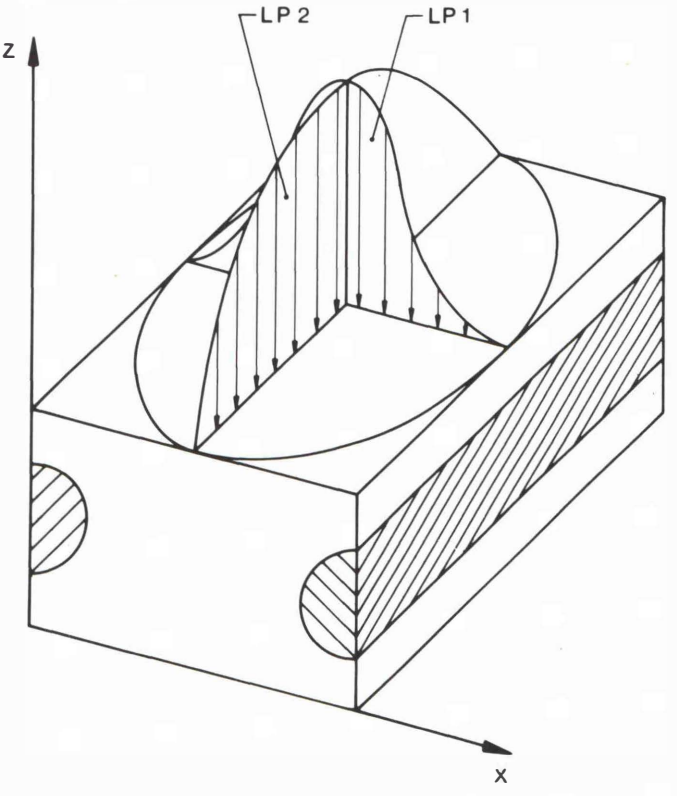

3.2 Stress and Deformation in the Cross-Section of a Steelcord Belt With and Without Breaker

Peak load levels in the belt occur because the impact of a sharp lump is concentrated in a small area of the belt.

This leads to load-profiles as displayed in Fig. 3.

A cut along one of the marked planes reduces three to two degrees of freedom. There are different opinions on the side of manufacturers and users of conveyor belts, whether breaker plies add to the service life of a belt equivalent to the higher cost [12—14].

There are different constructions of breakers, depending on the desired effect, which might mainly be protection against penetration or slitting.

The quantitative effect of a woven breaker ply on the distribution of stress and deformation of a steelcord belt, type ST 800, has been calculated with the use of the Finite-Element method. A non-linear approach, taking into consideration the non-linear effect of the value of deformation, is available in the Programme NASTRAN and has been conducted.

Fig. 4 shows a deformed cross-section of a ST 800 without a breaker ply.

Compared to a cross-section of same geometric data under the same load but with one breaker ply, Fig. 5, deformations

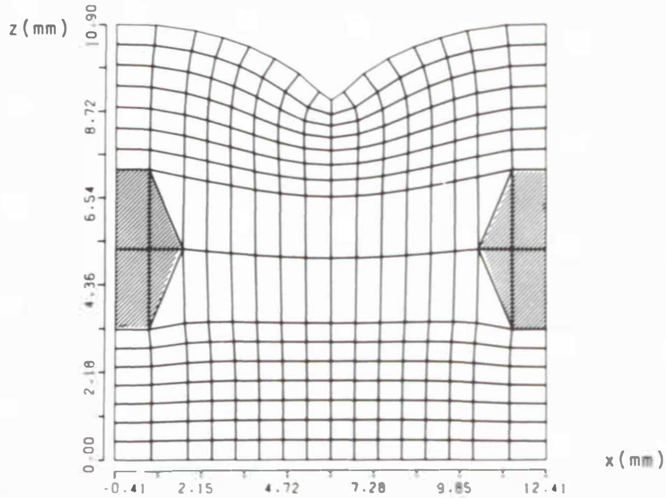

Fig. 4: Deformed cross-section of a steelcord belt ST 800 without breaker

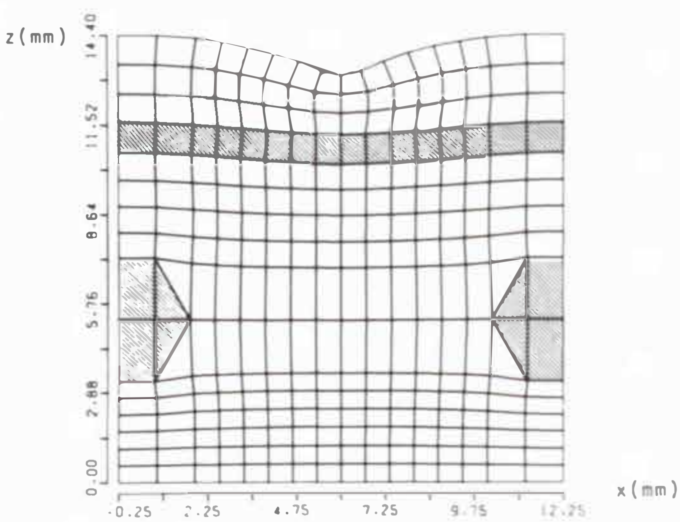

Fig. 5: Deformed cross-section of a steelcord belt ST 800 with breaker

below the breaker are substantially less. Distribution of stress becomes significantly more homogeneous, caused by the strength of the breaker ply in direction ∅ (see Fig. 3).

The Finite-Element approximation of a real continuum naturally leads to an error, whose upper limit cannot be determined, when a non-linear approach is made.

The reliability of these calculations had to be proven by the application of another method to the problem. Therefore the Finite-Differences method has been used to solve two non-linear partial differential equations, which are exact for large deformations of the even cross-section.

The equations result from an Euler description of deformation and read as follows:

$$
\begin{aligned}
&(\lambda + 2\mu)\,\{\,2\,(1 + u_x)\,(u_{xx} + u_x u_{xx} + v_x v_{xx}) + u_{xx}\,(2u_x + u_x^2 \\
&+ v_x^2) + 2u_y\,(v_{yy} + u_y u_{yy} + v_y v_{yy}) + u_{yy}\,(2v_y + u_y^2 + v_y^2)\,\} \\
&+ \lambda\,\{\,2\,(1 + u_x)\,(v_{xy} + u_y u_{xy} + v_y v_{xy}) + u_{xx}\,(2v_y + u_y^2 + v_y^2) \\
&+ 2u_y\,(u_{xy} + u_x u_{xy} + v_x v_{xy}) + u_{yy}\,(2u_x + u_x^2 + v_x^2)\,\} \\
&+ 2\mu\,\{\,2u_{xy}\,(u_y + v_x + u_x u_y + v_x v_y) + u_y\,(u_{xy} + v_{xx} \\
&+ u_{xx} u_y + u_x u_{xy} + v_{xx} v_y + v_x v_{xy}) + (1 + u_x)\,(u_{yy} + v_{xy} \\
&+ u_{xy} u_y + u_x u_{yy} + v_{xy} v_y + v_x v_{yy})\,\} = 0
\end{aligned}
$$

$$
\begin{aligned}
&(\lambda + 2\mu)\,\{\,2v_x\,(u_{xx} + u_x u_{xx} + v_x v_{xx}) + v_{xx}\,(2u_x + u_x^2 + v_x^2) \\
&+ 2\,(1 + v_y)\,(v_{yy} + u_y u_{yy} + v_y v_{yy}) + v_{yy}\,(2v_y + u_y^2 + v_y^2)\,\} \\
&+ \lambda\,\{\,2v_x\,(v_{xy} + u_y u_{xy} + v_y v_{xy}) + v_{xx}\,(2v_y + u_y^2 + v_y^2) \\
&+ 2\,(1 + v_y)\,(u_{xy} + u_x u_{xy} + v_x v_{xy}) + v_{yy}\,(2u_x + u_x^2 + v_x^2)\,\} \\
&+ 2\mu\,\{\,2v_{xy}\,(u_y + v_x + u_x u_y + v_x v_y) + (1 + v_y)\,(u_{xy} \\
&+ v_{xx} + u_{xx} u_y + u_x u_{xy} + v_{xx} v_y + v_x v_{xy}) + v_x\,(u_{yy} + v_{xy} \\
&+ u_{xy} u_y + u_x u_{yy} + v_{xy} v_y + v_x v_{yy})\,\} = 0
\end{aligned}
$$

Herein $\sqrt{\ }$ and * are assigned to the deformations in the direction of the ∅- and ‰-axis, $\sqrt{_x}, \sqrt{_{xx}} \ldots$ to the derivatives of first and second order.

For details concerning the Finite-Element method, Finite-Differences formula and related numerical problems one should consult the special literature [15, 16].

Convergency of the results of both methods becomes clear when deformations obtained with both methods, applied to the same problem, are plotted together.

Fig. 6 gives an example. Dotted lines stand for Finite-Element deformation continuous lines for Finite-Differences deformation.

4. Conveyor Belt Wear Test Stand

To study the influences which determine the wear of a belt, a wear test stand has been designed and built, which provides exactly known operating conditions of the belt, at the cost of unavoidable idealisations.

Belt wear in this sense is: "the process in which the conveyor belt becomes unfit for use during a certain minimum service life, which to a considerable extent results from, or is related to, continuous damage of the cover plates".

Fig. 7 shows a photograph of the test stand, which has been described in detail before [17]. The test stand consists of a normal conveyor, to which a loading device is added. This device comprises a test cylinder, equipped with 24 sharp edged impact test objects.

Fig. 7: Conveyor belt wear test stand

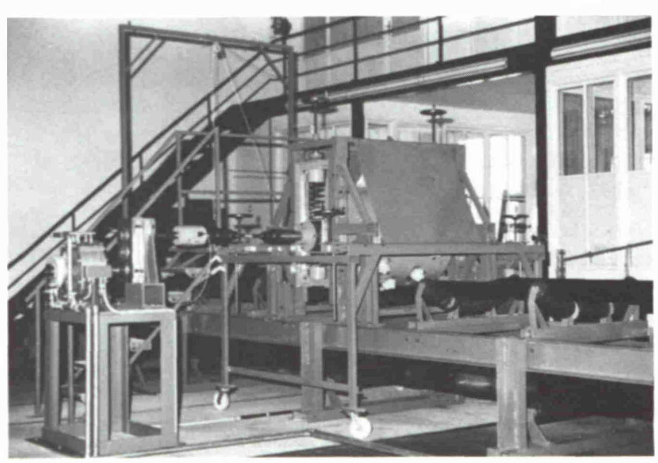

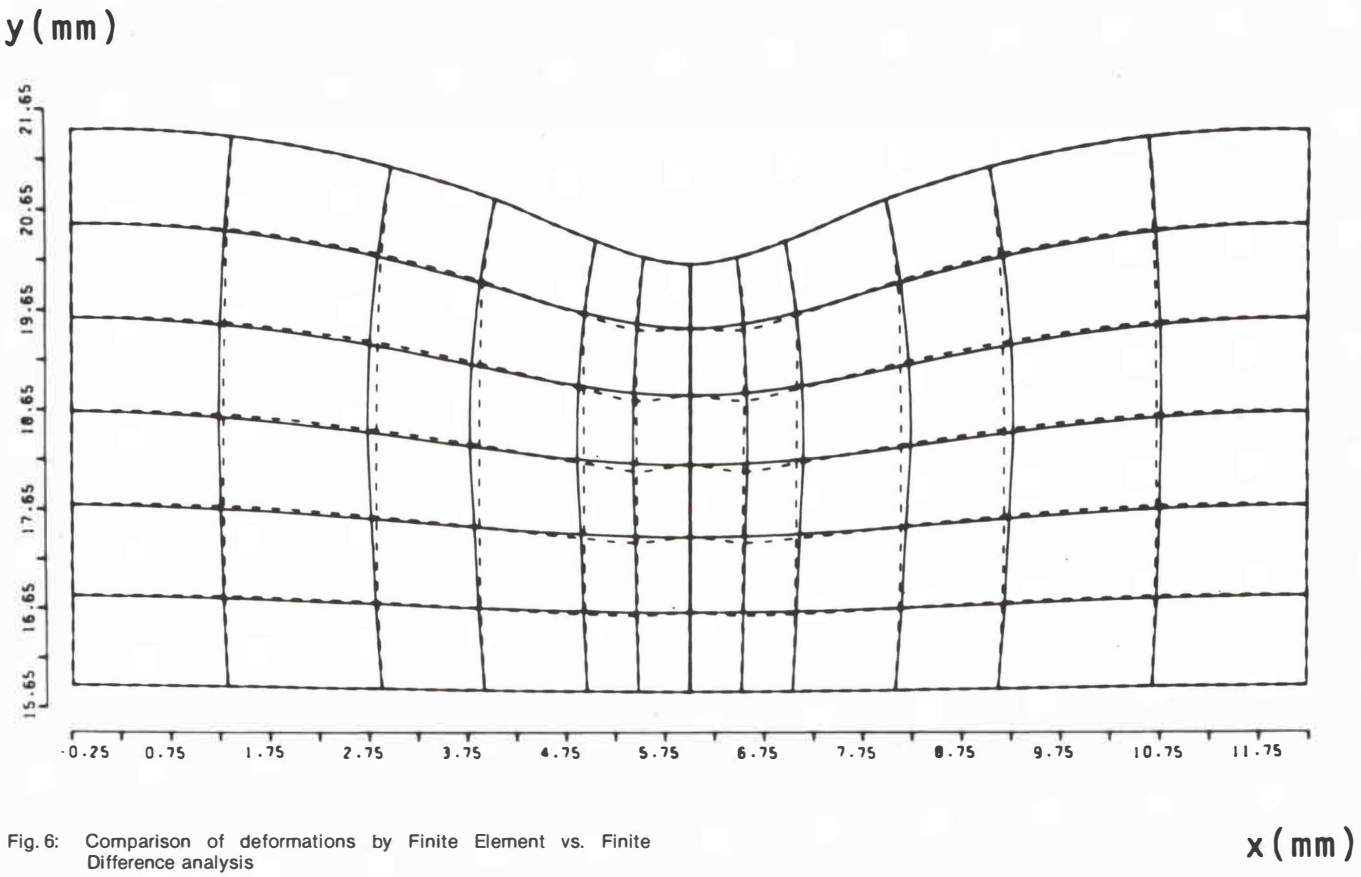

Fig. 6: Comparison of deformations by Finite Element vs. Finite Difference analysis

The main technical data of the wear test stand are:

center distance	11 m
belt width	800 mm
belt speed	0.0—5.0 m/s
power of hydrostatic drive	66 kW
power of eddy current brake	75 kW
pulley diameter	610 mm
test cylinder diameter	820 mm
initial tension (servo-hydraulic)	0—100 kN

The cylinder is passively driven by the running belt onto which it is pressed. A torque moment, simulating acceleration of lumpy pieces is applied by an eddy current brake.

Impulse forces on the tip of one of the test objects, moment of the brake, initial tension, belt speed and power consumption of the conveyor drive are measured and controlled during a test, which might take up to six weeks.

The test objects are made from steel-fibre reinforced concrete, because the surface of concrete is not smoothed during a test, but cracked, thus forming new micro-edges at a nearly constant rate.

The intention of the wear test stand has been to detect and quantify how the construction of the carcass and breaker influence the grade of wear and whether there is a coincidence of certain manifestations of wear with the type of the belt studied. In the long run, data obtained from the wear test stand should improve the design of impact belts and at least make it easier to predict the service life and expected cost of maintenance. As a side effect the significance of quality tests for the suitability of a belt could be much better rated.

5. Specific Abrasivity of Bulk Materials

According to Thomas [18], micro-edges determine the abrasion on a rubber surface in contact with a test object.

From that point of view, the physical and chemical properties of a lump do not influence the abrasion, provided there is a minimum hardness and roughness of the material, compared to rubber.

This has given grounds for an investigation of the surfaces of bulk materials such as gravel, limestone, sandstone, granite, ore, gypsum, marble and in addition corundum 60 and 100, and fibre concrete. Perthometer profiles, recorded from casts of the materials, have been evaluated in respect of the number of peaks per length. Fig. 8 gives an example. The profile of a test piece of corundum 60 is displayed.

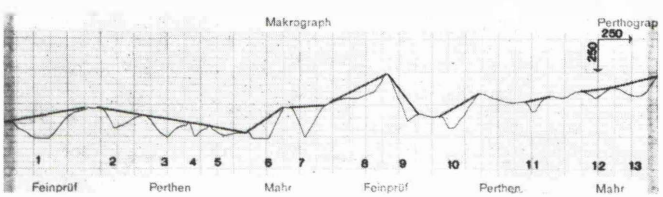

Fig. 8: Profile of corundum 60

A criterion R_p has been defined as follows.

$$R_p = \frac{n_p}{a_s} 1000 \left(\frac{1}{\mu}\right)$$

Herein the number n_p of classified peaks (e.g. greater than 50 μm) and the added length of the secants a_s are referred to.

This leads to a standard of abrasivity A_s, when the R_p-value of corundum 60 is set to 1.0.

Corundum 60 is used for abrasion resistance tests following DIN 53516 [21]. The specific abrasivity A_s of the said materials is listed in Table 1.

Table 1: Specific abrasivity of different bulk materials

Testpiece	R_p $(\frac{1}{\mu})$	Abrasivity A_s
Sandstone	2.48	1.51
Granite	2.28	1.39
Corundum 100	2.27	1.38
Marble	1.81	1.10
Corundum 60	1.65	1.00
Gypsum	1.33	0.81
Ore (Fe)	0.91	0.55
Concrete (test object)	0.88	0.54
Limestone	0.63	0.38

6. Scanning the Wear of the Covers

Up to now, a well regarded wear scanning method does not exist. An inductive technique proposed by Harrison [19] is only suitable for steel cord belts.

For the use on the conveyor belt test stand, a wear scanning technique must be independent of the construction of the belt. A newly introduced ultrasonic method, which has been described in Bulk Solids Handling, Vol. 2 (1982) [17], provides a direct contactless method to determine the increment of wear, even of the running belt. Fig. 9 is a photograph of a redesigned device. For operation the sensor is mounted above the surface to be monitored at a certain, limited, distance.

Fig. 9: Ultra-sonic scanning device

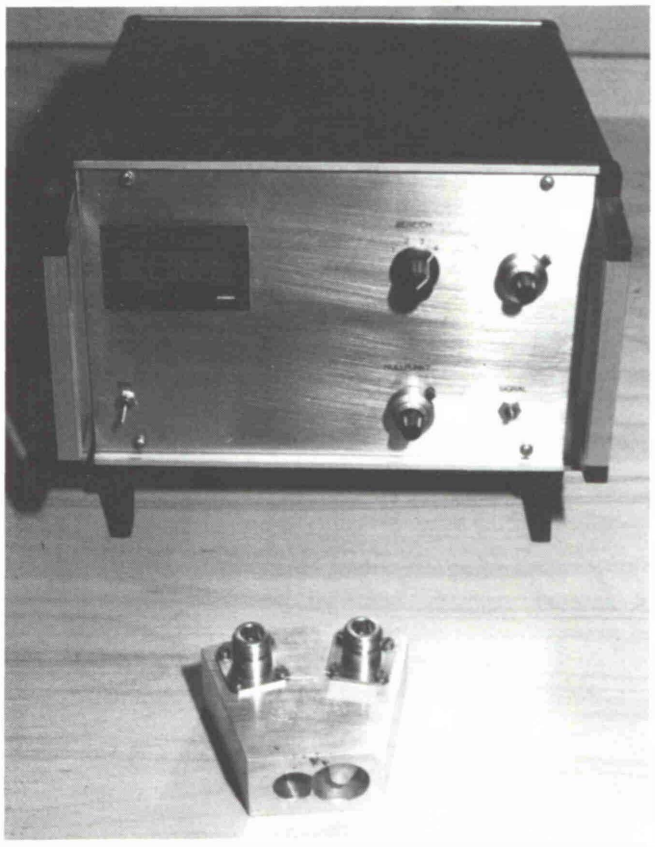

7. Results from the Wear Test Stand

7.1 Belts Under Test and Test Parameters

A first series of test runs was made to confirm the testing principle, the construction of the test stand and the ultrasonic scanning method and to find out correlations of belt design and wear increment.

Therefore a broad variety of belt types has been studied. Table 2 lists belts under test for the first series. Impact energy of the test objects has been equivalent to a lump of 30 kg striking the belt from 0.40 to 1.0 m of free fall. Impulse forces of the test objects as a function of time are, when considered as integral, equivalent to the impact of said lump, provided it hits between two idlers. Table 3 lists the test parameters.

7.2 Wear Increment Under Test Conditions

From the results of numerical calculation of stress and deformation in the cross-section of an EP 800 and a ST 800 belt, with and without breaker, different manifestations of wear had to be expected. Furthermore the higher elasticity and damping ratio of textile belts reduces peak levels of dynamic loads.

Wear profiles are recorded in regular intervals at marked reference lines on the belt. When evaluated, for example under the criterion of planimetric wear W_q, [20], the wear process can be quantified as a function of test time.

Fig. 10 shows a diagram in which the planimetric wear at three reference lines is plotted as a function of test cycles.

Fig. 10: Planimetric wear as a function of test cycles

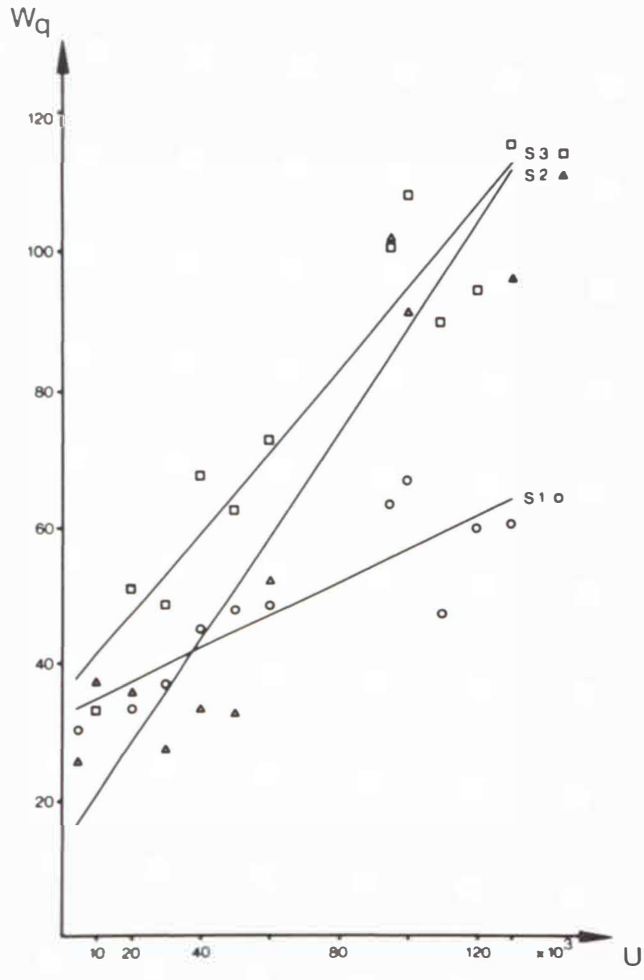

Table 2: Belts under test

Belt No.	Manufacturer	Tension member	Construction	Breaker	Rubber quality according to manufacturer	Thickness of cover (mm) bearing/running side
1	1	steelcord	ST 1000	no	M	4/2
2	2	steelcord	ST 1000	no	M and N	5/5
3	1	steelcord	ST 630X	no	N	3/3
4	1	polyester/ polyamide	EP 630/4	no	N	2/2
5	1	polyester/ polyamide	EP 1000/4	no	—	4/4
6	3	polyester/ polyamide	EP 800/3	steelcord 1 — layer	—	10/3
7	4	polyester/ polyamide	EP 1000/4	no	M and N	5/5
8	4	steelcord	ST 1000	no	M and N	5/5
9	1	steelcord	ST 1000	no	V	4/4
10	3	polyester/ polyamide	EP 1000/4	steelcord 2 — layers	—	9/3

Table 3: Test parameters

Belt No.	Initial tension	Belt speed (m/sec)	Brake torque (Nm) mean	Tangential-/Vertical peak forces mean
1	50	4.5	230	0.73
2	50	3.8	200	0.98
3	40	3.8	220	0.90
4	40	3.8	210	0.93
5	50	4.5	220	0.72
6	50	4.5	220	0.49
7	50	4.2	370	0.52
8	50	4.2	370	0.50
9	50	4.2	330	0.37
10	50	4.2	300	0.38

Table 4: Technological grade of wear GW_t of test belts

Belt No.	Belt width B (mm)	x_R	x_F	n_R	n_S	GW_t (%)
1	640	0.5	4.0	6	2	80.0
2	620	0.5	4.5	3	2	64.7/59.0
3	640	0.5	4.5	5	1	100.0
4	640	0.5	5.0	3	0	54.0
5	620	0.5	4.5	0	0	6.5
6	620	0.5	4.5	0	0	———*
7	640	0.5	4.0	0	0	4.1
8	640	0.5	4.5	10	0	46.5/42.0
9	640	0.5	4.5	8	0	43.8
10	630	0.5	4.0	0	0	3.7

*) accurate measurement not possible

7.3 Technological Grade of Wear

Different forms of wear, which have been observed and which evidently depend on the construction of the belt, make it necessary to define a criterion of wear which can be applied to any type of belt. With the help of this criterion, wear resulting from the same operating conditions can be rated. Thus different belt types can be compared to each other and a standard established by the test stand.

The criterion, which is named "Technological Grade of Wear", GW_t, is defined with respect to the effect of certain manifestations of wear on the reliability of a conveyor. It is evident, that deep longitudinal cracks and constant abrasion of the cover must be rated quite differently, even if they lead to the same loss of rubber.

For a steel cord belt the technological grade of wear reads as follows:

$$GW_t = \left(\frac{n_R t}{B \, x_R} + x_F \frac{\bar{d}_2}{d_t} + n_S \frac{d_1}{d_{ges}} \quad \frac{l_1}{B} \right) 100\ \%$$

For explanation of the symbols see Fig. 11. x_R and x_F are factors to be chosen by the user, depending on the reliability of the conveyor required, $\bar{d}_2$ is the mean of d_2.

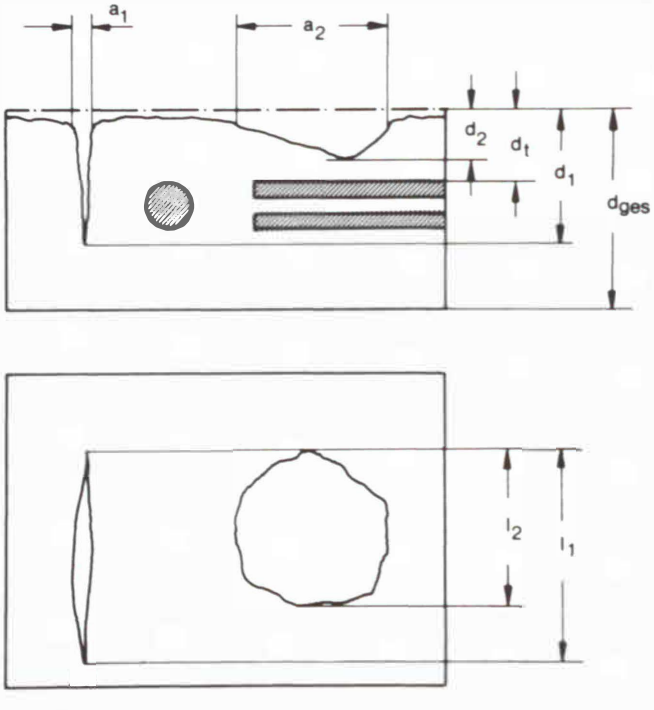

Fig. 11: Definition of the technological grade of wear

If applied to the first 10 belts under test, the criterion makes it evident that textile reinforced belts are better suited for conveyors with a short center distance under high loading point impact, e.g., belts for bucket wheel excavators, roughly by a factor of 10, see Table 4.

8. Experimental Results Compared to Numerical Calculations and the Literature

Maximum acceleration of a lumpy mass striking the belt at the loading point is a roughly linear function of the height of fall, which is not significantly influenced by the belt speed. Maier [2] reports a different relationship between peak forces and height of fall, which is a function of the square root type. One has to consider that in this investigation the test object was dropped onto completely constrained pieces of the belts. Micro-edges and their geometric data determine the abrasivity of any given material; shape and mass of a lump, the mean surface pressure. This has led to a direct definition of abrasivity of different materials, evaluated from surface scans. Abrasivity of an interesting material can thus be rated against K60, which is used for abrasion resistance tests according to DIN 53516 [21]. Results from the wear test stand are not comparable to other reports, because a similiar test stand does not exist. A technological grade of wear has been established to comprise different manifestations of wear, occurring even under the same operating conditions.

Further details introduced into this criterion, e.g., distribution of angles of cracks, scores and channels, should make it applicable to description of wear in underground or open pit operations.

Test stand results underline that wear cannot be defined solely from cracking and fatigue.

Distributions of stress, which have been calculated and for which high shear at the surface of the ropes and positive tensile tension in the direction of the x-axis are typical, are confirmed by experimental results. The technological grade of wear clearly indicates that textile reinforced belts are better suited for high impact conditions.

Steel-cord belts should be made with one or more breaker plies if significant impact is expected.

References

[1] Grimmer, K.-J., Thormann, D., "Zur Problematik der Kraft- und Bewegungsabläufe des Schüttguts an der Aufgabestelle von Förderbandanlagen", Fördern und Heben 4 (1967)

[2] Maier, H., "Vergleichende Untersuchung des Beaufschlagungsverhaltens von Gummifördergurten beim senkrechten Aufprall einer Einzelmasse", Dissertation, TU Hannover (1963)

[3] Oehmen, H., Alles, R., "Stoßkraftmessungen an Förderbandtragrollen und Untersuchungen der Durchgangsform von Fördergurten", Braunkohle, Wärme und Energie 12 (1972)

[4] Ballhaus, H., "Die Impulskräfte beim Aufprall grobstückigen Gutes auf den Fördergurt", Braunkohle 6 (1981) 184—187

[5] DIN 53504, "Bestimmung von Reißfestigkeit, Zugfestigkeit, Reißdehnung und Spannungswerten im Zugversuch"

[6] Mooney, M., "A Theory of Large Elastic Deformation", Journal of Applied Physics 9 (1940) 582—592

[7] Hart-Smith, L.J., "Elasticity parameters for finite deformations of rubber-like materials", Zeitschrift für angewandte Mathematik und Physik 5 (1966) 608—626

[8] Gohl, W., "Elastomere", Kontakt und Studium, Band 5, Akademie Esslingen (1978)

[9] Göbel, E.F., "Gummifedern", 3. Auflage, Springer Verlag, Berlin, Heidelberg, New York (1969)

[10] Kainradl, P., "Verformungseigenschaften von Vulkanisaten", Kautschuk und Gummi 10 (1957) 278—285 and 308—316; 11 (1958) 14—17

[11] DIN 22 131, "Fördergurte mit Stahlseileinlagen, Maße und Kennzeichnung, Güteanforderungen, Prüfung, Gurtverbindung"

[12] Lachmann, H.P., "Fördergurte, Aufwand und Verfügbarkeit", Braunkohle 6 (1981) 178—183

[13] Hartlieb von Wallthor, R., "Gurtförderung im Steinkohlenbergbau unter Tage unter besonderer Berücksichtigung der Probleme an Fördergurten", Braunkohle 6 (1979) 166—173

[14] Paul, F., "Querarmierung aus elastischen Stahldrahtlitzen erhöht die Durchschlagfestigkeit", Fördern und Heben 12 (1978) 847—850

[15] Zienkiewicz, O.C., "The Finite Element Method in Engineering Science", McGraw-Hill, London (1971)

[16] Marsal, D., "Die numerische Lösung partieller Differentialgleichungen", BI — Wissenschaftsverlag, Mannheim, Wien, Zürich (1975)

[17] Ballhaus, H., "A New Conveyor Belt Wear Test Stand", Bulk Solids Handling 2 (1982) 59—63

[18] Thomas, A.-G., "Factors Influencing the Strength of Rubbers", Rubber Chemical Technology (1975) 902—912

[19] Harrison, A., "Wear Profile Measurement of the Rubber Covers of Steel-Cord Belts", Australian Coal Miner 3 (1981) 38—41

[20] DIN 50320, "Verschleiß, Begriffe, Systemanalyse von Verschleißvorgängen, Gliederung des Verschleißgebietes", Beuth Verlag, Berlin, Köln, 12 (1979)

[21] DIN 53516, "Bestimmung des Abriebs" Beuth Verlag, Berlin, Köln

Acknowledgements

The author would like to express his gratitude to Prof. Dr.-Ing. E. Bahke, Director of the Institut für Fördertechnik der Universität Karlsruhe, for his interest in this work, which has been performed in the Institute.